

DETERMINING THE ABILITY TO USE DIRECT BROADCAST SYSTEM (DBS) DATA TO FORECAST SEVERE WEATHER

Anthony DiNorscia, Hampton University

William Smith, John McNabb, Hampton University

We research the capability of the direct broadcast system (DBS) received sounding radiance data for forecasting severe weather. This study is important for Hampton Roads because severe weather, such as flash floods and severe thunderstorms, is frequent in this area, and the DBS can lead to faster warnings. The DBS is located on top of the Harbor Center in Hampton, Virginia and collects data from satellites as they orbit within the line-of-sight of the receiving antenna. For this research, we focused on the Atmospheric Infrared Sounder (AIRS), Cross-track Infrared Sounder (CrIS), and Infrared Atmospheric Sounding Interferometer (IASI). These three instruments provide sounding data that produces a vertical profile of the atmosphere. The sounding data is compared to different meteorological data sets. These data sets include radiosonde data, Rapid Refresh (RAP) and High-Resolution Rapid Refresh (HRRR) model atmospheric profiles, and geostationary satellite Advanced Baseline Imager (ABI) data. We use statistics to understand how well the soundings created from the DBS hyperspectral radiances compare to the radiosonde, RAP, and HRRR data. We also combine ABI radiance derived sounding data with the DBS sounding data to create a data set that has the high vertical resolution provided by the DBS hyperspectral radiance observations and the much better spatial and temporal resolutions provided by the ABI multispectral radiance observations. The results show that the DBS closely matches the other meteorological data sets and combining the DBS data with the ABI data allows for more detailed and more frequent sounding data as required to improve severe weather predictions.

Introduction

Severe Weather in Hampton Roads

Severe weather is prevalent all around the globe, including Hampton Roads. These intense weather events can lead to deaths and millions of dollars in damage. Dating back to 1950, there have been 21 deaths, 363 injuries, and over 480 million dollars of damage caused by severe storms in the Hampton Roads area (NCDC 2018). With the improvement in technology, more people are warned earlier than before, even though there is still room for improvement. Forecasts can improve even more with better technology and more available data. The direct broadcast system (DBS) provides sounding data that shows how the atmosphere changes vertically, which depending on how it changes, can lead to being able to determine if the atmosphere is stable or unstable. Instability is a precursor for severe weather. Instability occurs when a

parcel of air is warmer than the atmosphere around it. This leads to the parcel rising, which also leads to the parcel expanding. As the parcel rises, it can become saturated, which leads to cloud formation. When the atmosphere is very unstable, or remains warmer than the surrounding air, the air parcel can rise to the tropopause, which leads to cumulonimbus clouds and extremely severe weather events. To forecast this instability in the atmosphere, two specific stability parameters can be used and are used widely in the forecasting community.

Two stability parameters that can be derived from sounding data are convective available potential energy (CAPE) and lifted index (LI). CAPE is the vertical integration of the buoyant energy contained in a parcel. Since CAPE does not have units of temperature, because it is joules/kilogram (J/kg), it is not truly a measure of stability (Blanchard 1998). Although, large numbers of CAPE are usually linked to an unstable

atmosphere, which has the potential to experience severe weather. The second parameter that is used to forecast severe weather is LI. This does have units of temperature and is found by calculating the difference between the temperature of the atmosphere surrounding the parcel and the parcel temperature and at around 500 millibars (mb). Negative LI values indicate instability and a value of -6° or less is very unstable (Galway 1956; DeRubertis 2006). Although CAPE and LI data will not be mentioned much in this research paper, these stability parameters can be and have been derived from sounding data that is measured using hyperspectral sounders and retrieved using the DBS.

Hyperspectral Sounders

Hyperspectral sounders are important for both research scientists and weather forecasters. They are called sounders because they measure radiance, which is used to solve for atmospheric vertical profiles, from top to bottom. They are described as hyperspectral because they observe thousands of spectral channels of radiance, which can provide very high vertical resolution. These hyperspectral sounders are currently onboard polar satellites, and are beginning to fly on geostationary satellites. Since the 1980s, they have been on aircrafts and since 2002, they have been spaceborne on satellites (Smith et al. 2009).

These sounders use different spectral channels to measure different atmospheric parameters. They do this by measuring the radiation upwelling from the surface and atmospheric emissions to the satellite instrument. A couple examples include carbon dioxide (CO_2) being used to determine temperature and water molecules being used to determine the moisture content of the air. The hyperspectral sounders used in this paper measure in the infrared (IR) region. The amount of radiation that is measured at certain

wavelengths can be used to determine a certain atmospheric parameter. An inverse form of the radiative transfer equation can be implemented to solve for the atmospheric parameters using the radiation spectrum measured by the sounders. Then, the altitude at which the radiation was emitted from, or the parameter was measured from, is determined by the weighting function. Using both the radiance measurement and the weighting function, measurements of different atmospheric parameters can be determined as a function of altitude (Smith et al. 1972). These measurements run into issues when clouds are present because of the fact that IR radiation is attenuated by clouds.

To solve for the issue of clouds, a dual-regression (DR) satellite sounding algorithm was created and explained by Smith et al. (2012) and Smith and Weisz (2017). This algorithm allows for data to be processed on both clear and cloudy field-of-view conditions. This DR algorithm computes two sets of regression coefficients offline using an ensemble of climatological data: one for clear cases and one for cloudy cases. These two sets of coefficients are then applied to the satellite-measured radiances to get a clear and cloudy retrieval. Then, the data is vertically de-aliased and bias corrected using model forecast data to allow for the most accurate form of the retrieval. After correcting any errors, it was found that the DR process could produce sounding results similar to radiosonde measurements (Smith and Weisz 2017). The three hyperspectral sounding instruments' data used for this research are all obtained using the DR algorithm.

DBS and Instruments

The DBS used for this research is in Hampton, Virginia on top of the Harbor Center. This DBS belongs to Hampton University and was installed on September 26, 2016 (Hampton University 2016). This DBS

is used to retrieve data from satellites as they pass within the line-of-sight of the DBS's antenna. Since the DBS has the ability to retrieve the data as soon as the satellite overpasses, the DBS data is considered to be real-time satellite data. This real-time data is important for severe weather forecasting. The DBS can gather data from any satellite passing within the line-of-sight of its antenna, but the DBS at Hampton prioritizes polar satellites. These polar satellites are prioritized because they include hyperspectral sounders. The hyperspectral sounder data that are used in this research and collected by the DBS come from the Atmospheric Infrared Sounder (AIRS), Cross-track Infrared Sounder (CrIS), and the Infrared Atmospheric Sounding Interferometer (IASI).

AIRS is in orbit on National Aeronautics and Space Administration's (NASA) Aqua satellite, which was launched in May 2002 and was the first hyperspectral IR sounder launched into space (Zheng et al. 2015). AIRS is a grating spectrometer type instrument, which has a spatial resolution of 13.5 kilometers (km) and a temporal resolution of about two times a day. Even though the spatial and temporal resolutions might be low, AIRS has 2378 spectral channels which result in high spectral resolution (Smith and Weisz 2017). AIRS has similar details as the other two instruments used.

CrIS is onboard both Suomi National Polar-orbiting Partnership (NPP) satellite and Joint Polar Satellite System (JPSS)-1 satellite, which were launched in October 2011 and November 2017, respectively (Smith and Weisz 2017; Glumb et al. 2018). CrIS is an example of a Michelson interferometer. This instrument has a spatial resolution of 14 km and the same temporal resolution as AIRS. Since CrIS is onboard two satellites, there are four overpasses instead of two. Being a hyperspectral sounder, the high spectral resolution is due to the 2211 spectral channels

(Smith and Weisz 2017; Wang et al. 2015). CrIS is the same instrument type as IASI.

IASI is also spaceborne on two separate satellites. Those satellites are Meteorological Operation (Metop)-A, launched in October 2006, and Metop-B, launched in September 2012. As mentioned earlier, IASI measures radiance the same way as CrIS because it is a Michelson interferometer as well. IASI has a relatively low spatial resolution of 12 km and it passes within line-of-sight of Hampton four times a day, two times for each satellite. Like CrIS and AIRS, IASI has high spectral resolution because it uses 8461 spectral channels (Smith and Weisz 2017). Details on all three instruments can be seen in Table 1. Using all three instruments are important because having satellite data at different times of the day can help diagnose how the atmosphere is changing.

Instrument	AIRS	IASI	CrIS
Type	Grating	Michelson	Michelson
Spectral Resolution (cm ⁻¹)	0.5-2.0	0.25	0.625(LW), 1.25(MW), 2.50(SW)
Spectral Range (cm ⁻¹)	650-2670	645-2760	650-2550
Detectors/channels	4756/2378	12/8461	27/2211
Spatial Resolution (nadir) (km)	13.5	12	14

Table 1. Instrument Details (Smith and Weisz 2017).

Project

This research is attempting to validate the capability of using the DBS to create severe weather forecasts. To do this, DBS data first needs to be validated along side other operationally-used forecasting tools and data sets. The DBS data used in this project consists of latitude, longitude, pressure levels, temperature, and dewpoint temperature. This data will be compared to the operationally-used data sets which consists of radiosonde data, Rapid Refresh (RAP) and High-

Resolution Rapid Refresh (HRRR) data, and Advanced Baseline Imager (ABI) data. These validations will show how well the DBS data is at producing accurate soundings of the atmosphere, which is important in determining if severe weather could occur.

Comparisons with Radiosonde Data

Data

Radiosondes are important instruments for forecasting weather. They are important because they make in-situ measurements, which mean they come into contact with what they are measuring. This is different from remote-sensing techniques, which consist of hyperspectral sounders, because remote-sensing measures parameters from space, which means they are a large distance away from the intended measured parameter. Using both in-situ and remote-sensing methods together can help determine errors in the methods and give a better picture of the atmosphere. Radiosonde data is the ground truth in this research because of the high-accuracy required by the World Meteorological Organization (2008). This data is collected by a radiosonde being raised in the atmosphere by a balloon and making measurements. Radiosondes, like hyperspectral sounders, measure atmospheric sounding data. The data used for the validation consists of temperature, and dewpoint temperature at different pressure levels of the atmosphere. The radiosonde data is downloaded from University at Wyoming at <http://weather.uwyo.edu/upperair/sounding.html>. Radiosondes run into spatial and temporal limitations because they are expensive to launch. They are mostly launched at 0 UTC and 12 UTC each day at National Weather Service (NWS) locations. For this research, the five closest NWS centers from Hampton were chosen. These locations include Blacksburg VA, Wallops Island VA, Sterling

VA, Greensboro NC, and Newport/Morehead City NC. Radiosondes can help validate the DBS data, but the DBS data can make measurements where and when radiosondes are not available.

Methodology

Comparing DBS data with radiosonde data is the most important validating technique used in this research due to the fact that radiosondes are very accurate and used for the ground truth. To do these comparisons, a couple of steps need to be completed. First, the DBS data and the radiosonde data are to be plotted onto a skew-t together. A skew-t diagram shows the temperature and dewpoint temperature data plotted vertically in the atmosphere, so they are commonly used when plotting sounding data. Second, statistics are calculated and plotted onto a statistical plot. These plots consist of the cumulative mean and cumulative standard deviations of the temperature and dewpoint temperature differences between the DBS and radiosonde data. These statistical plots will show the statistics at each level of the atmosphere.

The two data sets can be large distances away from each other since the radiosondes that are being used are from five locations around the area and, as mentioned earlier, the DBS data can be missing due to thick clouds. To assure that the comparisons are not large distances away, a 100 km limit is implemented for the data that is saved and plotted. This limit is important because of the spatial variability of temperature and, most important, moisture. The DBS and radiosonde data also are measured at different times, since the DBS overpass usually occurs in between the 0 UTC and 12 UTC radiosonde launches. Due to this temporal difference, both radiosondes are used to compare to each DBS overpass. An example of this skew-t comparison can be seen in Figure 1. The

statistical plots are computed for the DBS and both radiosondes.

The statistical plots are calculated using all of the current and previous data, meaning it is cumulative. There are three statistical plots used: the DBS compared to the radiosonde launched before the overpass, the radiosonde launched after the overpass, and an interpolated radiosonde that provides an estimate at the time of the overpass. These plots show the mean and standard deviation of the temperature and dewpoint temperature difference for each pressure level. An example of a cumulative statistical plot will be shown in the Comparison Results section.

Comparisons with RAP/HRRR Model Data

Data

The validation using RAP and HRRR models is important because these models are operationally used within the forecasting community. Also, the RAP model is used to de-alias the DBS retrievals, so it is especially important to see how the DBS data compares to the RAP model data. Finally, the RAP and HRRR are available where DBS is not due to clouds. These models use an ensemble of different data sets to get accurate model runs of the atmosphere. These data sets consist of data from surface observations, aircrafts, radiosondes, satellites, radars, and buoys (Benjamin et al. 2016). RAP has a spatial resolution of 13 km and HRRR has a spatial resolution of three km. Both models run every hour, so there will always be data that is available during a DBS overpass, unlike with the radiosonde data (Manikin et al. 2018). This data was retrieved from National Centers for Environment Prediction (NCEP) at <http://nomads.ncep.noaa.gov/>. The data from the models used for the comparisons include temperature, relative humidity, water vapor pressure, pressure levels, latitude, and longitude. The dewpoint temperature is

derived using the data retrieved from the model data. This data is important in validating the usage of the DBS data in forecasting weather.

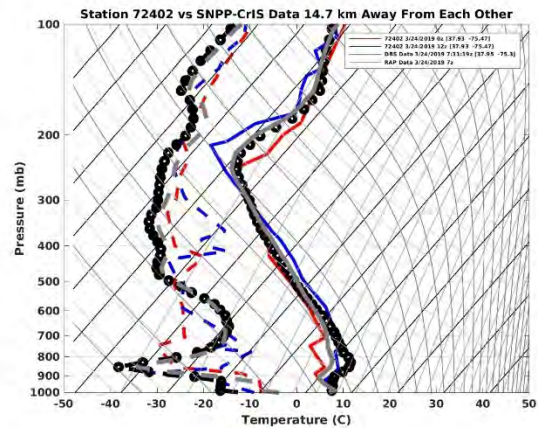


Figure 1. A skew-t comparison with Wallops Island VA 0 UTC (red line) and 12 UTC (blue line) data, RAP 7 UTC data (gray line), and CrIS DBS 7:31 UTC data (black line) on March 24, 2019.

Methodology

The comparisons between the DBS data and the model data follow a similar methodology as the radiosonde comparisons. This validation technique plots up the DBS alongside RAP data and HRRR data, and then plots up the cumulative statistics for the difference between the DBS and each model data set.

The difference between this comparison to the radiosonde comparison is that the RAP and HRRR data has a lot better coverage and is updated hourly. This means that there is no need for the distance limit nor multiple statistical plots, since there is always a model sounding near the DBS sounding at less than an hour difference than the DBS sounding. The RAP data is added onto the skew-t plot containing the radiosonde and the DBS soundings. An example of this RAP, radiosonde, and DBS sounding plot can be seen in Figure 1. The HRRR comparison plot consists of a HRRR sounding, RAP sounding, and the DBS sounding. RAP is added to all of the plots because that is the model data that is

used in the retrieval process of the DBS data, so it is important to see how both the DBS and RAP compare to the other data sets. An example of the HRRR comparison skew-t can be seen in Figure 2. The statistical plots for this validation technique use the RAP or HRRR data at the same time of the DBS data, so there is only one statistical plot used for each model. These plots can be seen in the Comparison Results.

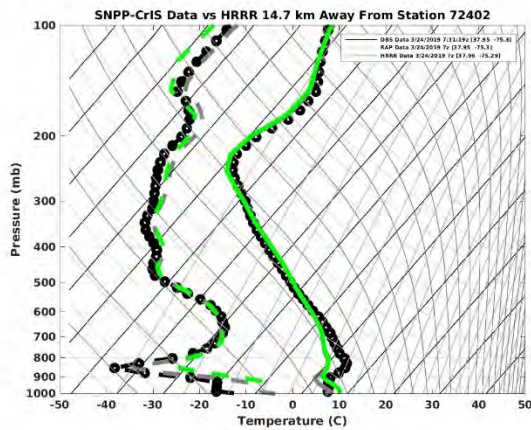


Figure 2. A skew-t comparison near Wallops Island VA using HRRR 7 UTC data (green line), RAP 7 UTC data (gray line), and CrIS DBS 7:31 UTC data (black line) on March 24, 2019.

Comparisons with PHSnABI Data

Data

The usage of ABI data in this project is different than the previously mentioned operationally-used data sets. The ABI data is actually combined, or fused, with the polar DBS data. This is done to increase the resolution in multiple ways. ABI is onboard the Geostationary Operational Environmental Satellite (GOES)-16 satellite, which was launched in November 2016. The spatial and temporal resolution of the ABI is much improved compared to the polar data collected by the DBS. The ABI has resolutions of 0.5 to two km and five minutes, respectively (Schmit et al. 2017). The data is retrieved at <ftp://ftp.ssec.wisc.edu/DR/ABI/>, which is provided by the University of Wisconsin. The

data has an increase in spatial and temporal resolution because the instrument is positioned over the same area being onboard a geostationary satellite. The downfall of the ABI instrument is that it has a lower spectral/vertical resolution due to only having 16 spectral channels. The higher spatial and temporal resolution from the ABI and the higher spectral/vertical resolution from the polar data is the reason behind fusing the ABI data and polar hyperspectral sounder (PHS) data. High resolution in all four dimensions is important in forecasting severe weather.

Combining the two sets of data is explained in detail by Weisz et al. (2017). This method uses data fusion to create PHS and ABI (PHSnABI) data sets. To briefly summarize the fusion technique, the five closest PHS field-of-views to each ABI pixel are averaged together to produce the best estimate of the high spectral resolution PHS sounding that would be observed at the high horizontal resolution ABI sounding location. This technique creates the PHSnABI data set that has PHS-like spectral resolution and ABI-like horizontal resolution. Once the PHSnABI files are created, they get compared to radiosonde and RAP data just like the PHS data, also known in this project as DBS data. The data used from these PHSnABI files to complete the comparisons include temperature, dewpoint temperature, pressure levels, latitude, and longitude.

Methodology

Similar to the previous two methods, the PHSnABI data is compared to both radiosonde and RAP model data by being shown together on a skew-t diagram. The PHSnABI data is plotted first, followed by the radiosonde and RAP data. An example of this skew-t plot can be seen in Figure 3. The five radiosonde locations mentioned earlier are still used for these comparisons. Since ABI data is produced every five minutes, the PHSnABI

data can be produce hourly. This leads to comparing PHSnABI data being available at 0 UTC and 12 UTC, which is the time of the radiosonde launches. There is still need of a 100 km limit, because the PHSnABI data can still have gaps due to clouds. There are two statistical plots created using PHSnABI data. The first plot is PHSnABI soundings compared to radiosondes. The second is PHSnABI soundings compared to the RAP model profiles. Each plot shows the mean and standard deviation of the temperature and dewpoint temperature difference between the PHSnABI data and radiosonde or RAP data at the different levels in the atmosphere. As mentioned earlier, these cumulative statistical plots will be shown in the Comparison Results section.

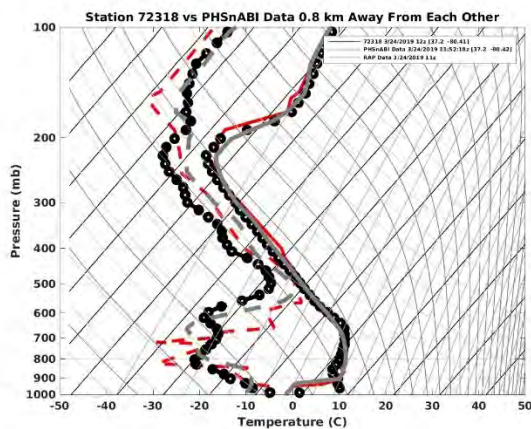


Figure 3. A skew-t comparison with Blacksburg VA 12 UTC data (red line), RAP 11 UTC data (gray line), and PHSnABI 11:52 UTC data (black line) on March 24, 2019.

Comparison Results

Radiosonde Comparisons

The radiosonde comparisons were done for all three instruments: CrIS, IASI, and AIRS. For this research paper, the results for CrIS will be shown because all three instruments show similar statistics. The statistics shown use each radiosonde comparison since March 2018. For CrIS, this means the statistics are cumulative and used

about 800 files. Each file includes the temperature and dewpoint temperature difference (CrIS - Radiosonde) at each of the five radiosonde locations. Where the distance is larger than 100 km or there is bad data due to temporal or spatial variability, the data is considered to be missing and not-a-number (NaN) is used. The mean and standard deviation for all of the cases are calculated. This data is then plotted vertically to show the mean and standard deviation of the temperature and dewpoint temperature at each level in the atmosphere. These cumulative statistical plots use blue lines for the mean differences and orange lines for the standard deviation of the differences. The first plot, which can be seen in Figure 4, shows the statistics for the CrIS (DBS data) compared to the radiosondes that were launched before the overpasses of CrIS. In this plot, the mean temperature difference hovers around zero. From the surface to about 800 mb, the difference is at most -0.5 Kelvin (K), which indicates that the radiosonde is warmer near the surface, and from about 400 mb to 200 mb, the DBS is warmer by about 0.5 K. The standard deviation for the temperature difference is at most 2.4 K and hovers around 1.5 K for most of the atmosphere. This indicates that the radiosondes and DBS are about +/- 1.5 K with temperature for most of the atmosphere, besides the surface which is about 2.5 K. This is a positive result due to the fact that radiosondes are very accurate and reliable in-situ measurements, and the DBS data is closely matching that accurate data. The dewpoint differences are larger compared to temperature, but this is due to the small-scale spatial and temporal variability of moisture in the atmosphere. With the radiosondes being different times and sometimes different locations, this can lead to a large difference in the moisture measurement between the radiosonde and CrIS. Moisture is used to calculate dewpoint temperature. Even with this variability, the

mean is between negative four and four K, which is a good result for this comparison. The DBS data has a colder dewpoint around 800 mb but the radiosonde is colder in the upper atmosphere. The standard deviation is where the variability is shown. Near the surface, it is around four degrees, but the middle of the atmosphere shows standard deviations around 12 K. This larger variability could be due to the presence of clouds and the temporal/spatial differences. A radiosonde can go through a cloud, which would have high levels of moisture, and CrIS sounding could be covering an area with no clouds, so a much lower dewpoint, or the opposite with a cloudy CrIS sounding and a clear radiosonde sounding. The statistics for CrIS compared to the radiosonde launched after the overpass and CrIS compared to the radiosonde estimated at the time of the overpass show similar results to the before overpass statistics.

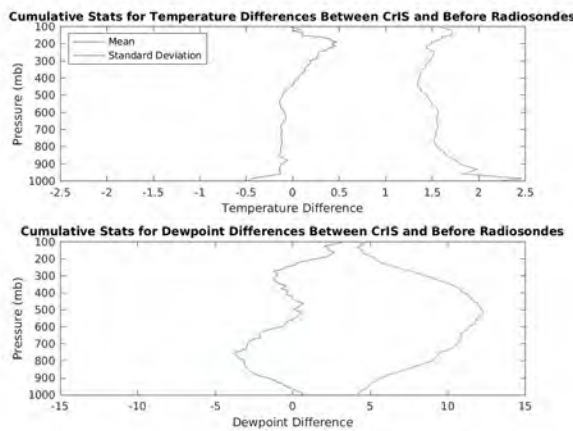


Figure 4. The cumulative statistics for the temperature and dewpoint temperature differences between CrIS and radiosondes that were launched before the DBS overpass. The mean differences (blue line) and the standard deviation of the differences (orange line) are plotted up for each altitude.

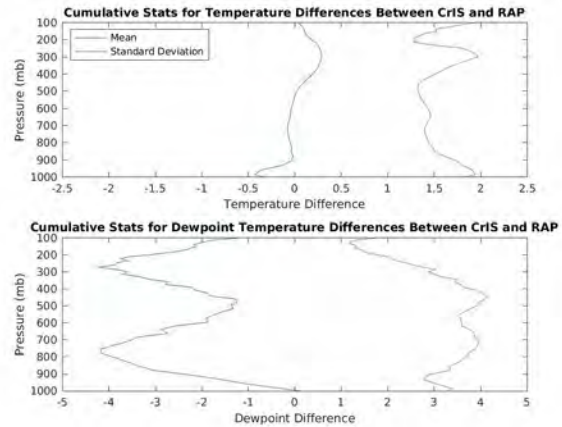


Figure 5. The cumulative statistics for the temperature and dewpoint temperature differences between CrIS and RAP.

RAP/HRRR Model Comparisons

The validation with the model comparisons was done to compare the DBS to forecasting models that are already being used operationally, and to compare the DBS data to the RAP, which is used as a-priori data and to correct the vertical structure of the DBS retrievals. The goal is to be as accurate or more accurate compared to the model data. Since the RAP and HRRR models run every hour, there is always data at or near an overpass. This leads to only needing one statistical plot for each model. The comparison with RAP can be seen in Figure 5. These statistics are created the same way as the radiosonde comparisons, except the differences are calculated using CrIS - RAP. There were about 800 cases for these as well, dating back to March 2018. Looking at these statistics, the mean temperature difference hovers around zero. The standard deviation is between 1.9 and 1.4 K. This shows that the DBS and RAP are in good agreement with respect to temperature throughout the atmosphere. The dewpoint temperature shows the variability due to the moisture variability in the atmosphere. The mean is negative the whole atmosphere, with the highest mean being negative four K. This is an indication that CrIS produces lower temperatures

throughout the atmosphere. The standard deviation is between one and four, which shows some variability, but still shows relatively close results when comparing CrIS to an operationally-used forecasting model. The HRRR comparison (not shown) has similar statistics to the RAP comparison. This is due to the fact that HRRR uses RAP model runs in its model.

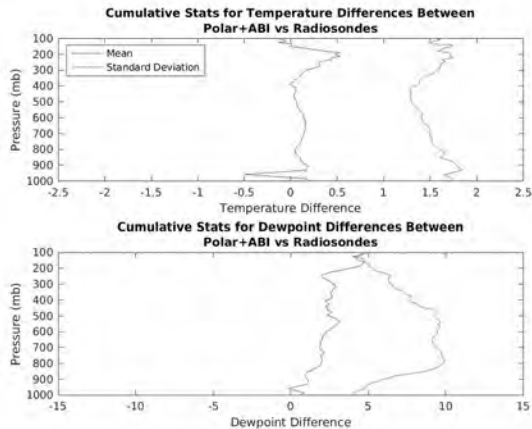


Figure 6. The cumulative statistics for the temperature and dewpoint temperature differences between PHSnABI and radiosondes.

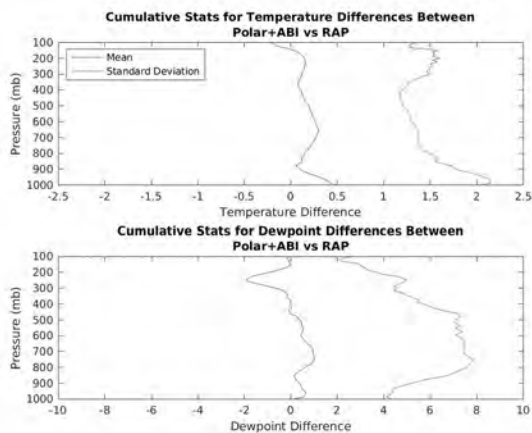


Figure 7. The cumulative statistics for the temperature and dewpoint temperature differences between PHSnABI and RAP.

PHSnABI Comparisons

Combining the PHS and ABI data is an important step in creating a severe weather forecasting tool because the combined data set can be produced hourly, or even less, and with

high horizontal and vertical resolution. These three things are needed because severe weather can be random and can end as quickly as it began. Comparing the PHSnABI data to radiosondes and the RAP model is done to validate that this combined data is as accurate or more accurate as these other forecasting tools. There are around 440 cases using PHSnABI files, which is less than the PHS-only cases because these comparisons started around June 2018. Unlike the PHS data, which had to be compared to the before and after-overpass radiosondes, the PHSnABI files are created hourly and can be compared to a specific radiosonde. This leads to the statistical plot of the PHSnABI - radiosonde temperature and dewpoint temperature differences at the same hour. This plot can be seen in Figure 6. The PHSnABI shows similar temperature results as the PHS data when compared to radiosondes. The mean temperature difference is between +/- 0.5 K and the standard deviation is at most 1.7 K. The dewpoint comparisons actually show better results with the PHSnABI. The mean dewpoint difference is between zero and five, so unlike the PHS data, the PHSnABI produces warmer dewpoint temperatures than the radiosondes from the surface to the top of the atmosphere. The standard deviation is at most 10 K, which is at the middle of the atmosphere and could be due to spatial variability of moisture due to clouds. Overall, the PHSnABI is shown to be as accurate or even more accurate than the PHS data and this could be due to using radiosondes at the same time and also the better horizontal resolution of the PHSnABI data. In Figure 7, the statistics for PHSnABI compared to the RAP model (PHSnABI - RAP) can be seen. In both the temperature and dewpoint temperature statistics, the mean is hovering around zero. The standard deviation of the temperature difference is at most two which is at the surface and hovers around 1.5 for the rest of the atmosphere. The standard deviation of the

dewpoint temperature difference is between two and eight K, with the maximum difference occurring in the middle of the atmosphere.

Discussion

The comparisons between CrIS data and operationally-used data sets showed positive results. These comparisons are also done with IASI and AIRS and they show similar results. It was shown that the temperature soundings between the DBS and radiosondes or RAP/HRRR model were closely matched with the a temperature difference no more than three K from the surface to the top of the atmosphere. This is an indicator that the DBS data can be used alongside these other tools to improve forecasts of the atmosphere. Even with the dewpoint difference being more variable, they were at most 12 degrees different between the compared soundings. This large difference also occurred in the middle of the atmosphere where clouds form, and with spatial and temporal differences, these clouds can cause a large difference between a cloudy sounding and a clear sounding. Although there is a larger difference in dewpoint temperature, the DBS data shows optimistic results and the ability of the DBS to produce accurate soundings of the atmosphere. The PHSnABI data set showed similar results for temperature and better results for dewpoint temperature. This is a great indicator that the higher-resolution PHSnABI data, which can be produced hourly, is as accurate or even more accurate than the DBS PHS-alone data. This is important in forecasting severe weather due to randomness of these storm events. Overall, the DBS data alone, and combined with ABI data, showed results that point to the data being able to perform as well or better than already used operational tools. This is important because the end goal of this research is to have these data being used operationally by the NWS centers. The

importance of better forecasting severe weather is increasing because even to this day, with the increase in technology, more and more people are injured or killed by these severe weather events, and this DBS data can hopefully increase warning times to help save more lives.

The future work for this project consists of adding this DBS and PHSnABI data to forecast models. This is where the main difference between the RAP model and the DBS data will be seen. Using the statistics is harder to show that the DBS is better because it uses the RAP data to create a better sounding of the atmosphere, but the comparison between severe weather forecasts will show which one does a better job at forecasting the events.

Acknowledgments

This research was supported under grant NASA CA-NNX15AQ03A (HU:CARE). The author would like to thank HU:CARE, Hampton University, and the Center of Atmospheric Science for the funding and the continuous help throughout this research. The author would also like to thank Dr. William Smith and Dr. John McNabb for their advisement with and contributions to this research. Finally, a special thank you goes out to the Virginia Space Grant Consortium for their funding through the Graduate STEM Research Fellowship Program and an opportunity to present this research at their annual conference.

- Benjamin, S. G., and Coauthors, 2016: A North American hourly assimilation and model forecast cycle: The Rapid Refresh. *Mon. Wea. Rev.*, **144**, 1669–1694, doi:<https://doi.org/10.1175/MWR-D-15-0242.1>
- Blanchard, D. O., 1998: Assessing the Vertical Distribution of Convective Available Potential Energy. *Wea. Forecasting*, **13**, 870–877, doi:10.1175/1520-0434(1998)013<0870:ATVDOC.2.0.CO;2
- DeRubertis, D., 2006: Recent Trends in Four Common Stability Indices Derived from U.S. Radiosonde Observations. *J. Climate.*, **19**, 309–323, doi:10.1175/JCLI3626.1
- Galway, J. G., 1956: The lifted index as a predictor of latent instability. *Bull. Amer. Meteor. Soc.*, **37**, 528–529.
- Glumb, R., L. Suwinski, S. Wells, A. Glumb, R. Malloy, and M. Colton, 2018: The JPSS CrIS Instruments and the Evolution of Space-Based Infrared Sounders. Accessed 24 March 2019. [Available online at <https://ntrs.nasa.gov/archive/nasa/casi.ntrs.nasa.gov/20180000526.pdf>]
- Hampton University, 2016: Hampton University Implements Direct Broadcast Weather Antenna. Accessed 8 Jan. 2018. [Available online at <http://news.hamptonu.edu/release/Hampton-University-Implements-Direct-Broadcast-Weather-Antenna>]
- Manikin, G., and Coauthors, 2018: RAPID REFRESH (RAP) Upgrade V4.0.0 HIGH RESOLUTION RAPID REFRESH (HRRR) Upgrade V3.0.0. Accessed 24 March 2019. [Available online at <https://rapidrefresh.noaa.gov/pdf/HRRRv3-RAPv4-CCB.pdf>].
- NCDC, 2018: Storm Events Database. Accessed 20 Jan. 2019. [Available online at <https://www.ncdc.noaa.gov/stormevents/>].
- Schmit, T. J., P. Griffith, M. M. Gunshor, J. M. Daniels, S. J. Goodman, and W. J. Lebar, 2017: A closer look at the ABI on the GOES-R series. *Bull. Amer. Meteor. Soc.*, **98**, 681–698, <https://doi.org/10.1175/BAMS-D-15-00230.1>
- Smith, W. L., H. M. Woolf, and H. E. Fleming, 1972: Retrieval of atmospheric temperature profiles from satellite measurements for dynamical forecasting. *J. Appl. Meteor.*, **11**, 113–122.
- Smith, W. L., H. Revercomb, G. Bingham, A. Larar, H. Huang., D. Zhou, J. Li, X. Liu, and S. Kireev, 2009: Evolution, current capabilities, and future advances in satellite nadir viewing ultra-spectral IR sounding of the lower atmosphere. *Atmos. Chem. Phys.*, **9**, 5563–5574, doi:10.5194/acp-9-5563-2009
- Smith, W. L., E. Weisz, S. V. Kireev, D. K. Zhou, Z. Li, and E. E. Borbas, 2012: Dual-regression retrieval algorithm for real-time processing of satellite ultraspectral radiances. *JAMC*, **51**, 1455–1476.
- Smith, W. L. and Weisz, E., 2017: Dual-Regression Approach for High-Spatial-Resolution Infrared Soundings. *Reference Module in Earth Systems and Environmental Sciences*. doi:10.1016/B978-0-12-409548-9.10394-X
- Wang, L., Y. Han, X. Jin, Y. Chen, and D. A. Tremblay, 2015: Radiometric consistency assessment of hyperspectral infrared sounders. *Atmos. Meas. Tech.*, **8**, 4831–4844, doi:10.5194/amt-8-4831-2015
- Weisz, E., B. A. Baum, and W. P. Menzel, 2017: Fusion of satellite-based imager and sounder data to construct supplementary high spatial resolution narrowband IR radiances, *J. Appl. Remote Sens.* **11**, 036022 (2017), doi: 10.1117/1.JRS.11.036022
- World Meteorological Organization, 2008: Guide to Meteorological Instruments and Methods of Observation; WMO-No. 8. Accessed 24 March 2019. [Available online at <https://www.weather.gov/media/epz/mesonet/CWOP-WMO8.pdf>].
- Zheng, J., J. Li, T. J. Schmit, J. Li, and Z. Liu, 2015: The impact of AIRS atmospheric temperature and moisture profiles on hurricane forecasts: Ike (2008) and Irene (2011). *Adv. Atmos. Sci.*, **32**, 319–335, <https://doi.org/10.1007/s00376-014-3162-z>